Influence of Added Salt on Chain Conformations in Poly(ethylene oxide) Melts: SANS Analysis with Complications

Shuyi Xie,[1] Bo Zhang,[2] Yimin Mao,[3,4] Lilin He,[5] Kunlun Hong,[6] Frank S. Bates,[2] and Timothy P. Lodge*[1,2]

[1]Department of Chemistry and [2]Department of Chemical Engineering and Materials Science, University of Minnesota, Minneapolis, MN 55455

[3]Department of Materials Science and Engineering, University of Maryland, College Park, MD 20742

[4]NIST Center for Neutron Research, National Institute of Standards and Technology, Gaithersburg, MD 20899

[5]Neutron Scattering Division, and [6]Center for Nanophase Materials Science, Oak Ridge National Laboratory, Oak Ridge, TN 37831

Author for correspondence: lodge@umn.edu

TOC graphic

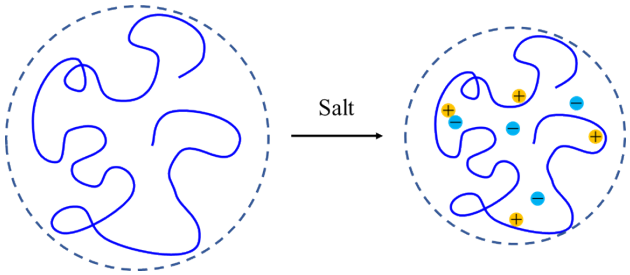

ABSTRACT

Poly(ethylene oxide) (PEO)-based electrolytes have gained increasing attention in both the rechargeable battery industry and fundamental research, but any influence of the ions on the polymer conformation is not fully understood. Small-angle neutron scattering (SANS) is a powerful means to determine single polymer chain conformations. We conducted SANS experiments on 50:50 blends of dPEO and hPEO of two different molecular weights (20 kDa and 40 kDa) doped with two different salts (LiTFSI and $LiClO_4$) at various concentrations. An additional measurement with LiI is also reported. Scattering profiles of salt-doped dPEO/hPEO blends were measured, and the incoherent scattering from dPEO and hPEO doped with salt was measured separately. A strong low q upturn was observed in some of the blends and in the pure dPEO homopolymers. The statistical segment lengths of PEO-salt mixtures were derived using a Kratky analysis. The segment length decreases modestly with increasing amounts of LiTFSI, but apparently first increases then decreases with added $LiClO_4$. At the highest salt concentration examined (r = $[Li^+]/[EO]$ = 0.125), a roughly 10% decrease in statistical segment length was observed in both LiTFSI and $LiClO_4$-doped PEOs, for both molecular weights. This work confirms that added salt causes a contraction of the PEO chain dimensions, but the effect appears slightly weaker than reported recently. Certain difficulties in data analysis are also discussed, including the unexplained low q scattering even in pure deuterated polymers, uncertainties in background subtraction, and inappropriate application of the Debye function.

INTRODUCTION

Ion-containing polymers are gaining increasing research interest for many applications, including fuel cells, lithium ion batteries, and water treatment membranes.[1] The most commonly investigated systems are electrolytes based on poly(ethylene oxide) (PEO), due to the strong ion dissociation and rapid segmental motion in the amorphous state. Ions can be introduced by adding ionic species directly (e.g., salts or ionic liquids (ILs)) or functionalizing the polymer backbone with charged groups.[2–6] In this way ion-conducting polymers can be engineered to enhance both the ionic conductivity and the ion transport selectivity. Moreover, the added charges may induce micro- or macro-phase separation in block copolymer or polymer blends, respectively, by increasing the segregation strength, which can result in the formation of novel nanostructures.[7–12] To understand phase behavior for such systems, and ultimately to optimize ion transport, any effect of added ions on polymer conformations, and possible "crosslinking" of chains by association with specific ions, needs to be better understood. However, the picture is still not clear, even in the apparently simple case where the PEO homopolymer is solvated by ILs or doped with salt. For example, PEO in imidazolium-based ILs exhibits an unusual LCST-type phase separation, partly due to the hydrogen bonding between the acidic proton of the imidazolium and the ether oxygen in PEO.[13,14] This hydrogen bonding effect contributes to the relatively good solubility of PEO in ILs. Small-angle neutron scattering (SANS) experiments show that in multiple ILs, the excluded volume exponent v, lies between 0.55 and 0.6, and the infinite dilution radius of gyration (R_g) is moderately larger than in the PEO melts.[15,16] Interestingly, hydrogen bonds with PEO are not always necessary to solvate PEO; for example, lithium tetraglyme bis(trifluoromethane) sulfonimide ([Li(G4)]TFSI) can solvate PEO due to Li^+/PEO coordination.[17,18] This coordination, sometimes considered as a transient cross-linking effect, is more apparent in PEO/salt mixtures. A crown ether-like conformation of PEO has been proposed, as evidenced by infrared and Raman spectroscopy and molecular dynamics (MD) simulations, which results in a decreased coil size.[19,20] More specifically, R_g values of neat and salt-doped PEO melts have been studied both by

simulations and experiments. By adding LiI at a salt concentration $r = [Li^+]/[EO] = 0.067$, Borodin and Smith found that R_g decreases by *ca.* 15%,[21] while Annis et al. found the decrease to be *ca.* 13% using MD simulations (M = 530 Da).[22] For the same system, Triolo, et al. only observed a slight decrease (*ca.* 3%) in R_g for LiI-doped PEO by SANS (M = 25,000 Da).[23] In comparison, Annis et al. observed a *ca.* 9% decrease by SANS for $M \approx$ 25,000 Da.[22] Recently, Loo et al. conducted a more systematic study of LiTFSI-doped PEO with M = 35,000 Da, and found that R_g decreases linearly with salt addition in the range $0 < r < 0.125$, but then the trend reverses, and R_g increases linearly at higher salt concentrations.[24] At $r = 0.067$, the decrease is 10%, which agrees well with the results from Annis, et al.[22] Kamiyama et al. studied the PEO conformation (M = 600 Da) when solvated in LiTFSI/IL and also observed an apparent decrease in R_g.[25] Collectively, it appears that the addition of salt induces a contraction of the PEO random coil, but to different degrees, depending on the type of the salt, salt concentration, and research method.

Here we report a systematic experimental study of the chain conformation of PEO of two different molecular weights (20 kDa and 40 kDa) doped with two different salts (LiTFSI and $LiClO_4$) at various concentrations. The statistical segment length, $l = (6/N)^{1/2}R_g$, is determined by SANS using a Kratky analysis. At the highest salt concentration (r = 0.125), a roughly 10% decrease in statistical segment length was observed in both LiTFSI and $LiClO_4$-doped PEOs, for both molecular weights. Where concentrations overlap, there is a reasonable qualitative agreement with Loo, et al.,[24] and Annis, et al.,[22] but the net effect of salt on PEO chain contraction appears to be slightly weaker. We also report a single measurement for LiI, to compare with the literature. We also report and discuss difficulties in data analysis, due to both unexplained upturns at low scattering wavevector q ($q = 4\pi \sin\theta / \lambda$, with θ being the scattering angle and λ the wavelength) in pure polymers and in certain blends, and to uncertainties in the incoherent contribution at high q. A Kratky analysis is chosen to minimize these effects.

EXPERIMENTAL SECTION

Materials. LiTFSI (3M) and $LiClO_4$ (Sigma-Aldrich) were dried under dynamic vacuum for 24 h at 120 °C and then stored in a glove box under argon. Two sets of hydrogenous PEO (hPEO) and deuterated PEO (dPEO) of two different molecular weights (20 kDa and 40 kDa) were synthesized via living anionic polymerization of hydrogenated and deuterated ethylene oxide (Sigma-Aldrich), respectively, using established air-free techniques.[26] Potassium *tert*-butoxide was used as the initiator, and the reaction was terminated with methanol. All PEO samples were precipitated in hexanes and redissolved in acetonitrile and filtered through a PVDF membrane with a pore size of 0.22 μm. After evaporating the solvent, samples were dissolved in HPLC water and dialyzed for 72 h before being freeze-dried. The molecular weights and dispersities ($Đ$) of the synthesized polymers (Table 1) were determined by size-exclusion chromatography (SEC) equipped with a Wyatt Optilab rEX refractive index detector and a Wyatt DAWN DSP multiangle laser light scattering (MALS) detector in tetrahydrofuran (THF) at 25 °C (Figure S1). A refractive index increment (dn/dc) of 0.068 and 0.057 mL/g was used for hPEO and dPEO, respectively.[15,27]

Table 1. Polymer Characteristics.

Component	M_n (kg/mol)[a]	$Đ = M_w/M_n$[a]	N[b]	Deuteration Conv. (%)[c]	ρ (g/mL)[d]
hPEO (20 kDa)	$20._5$	1.03	465	-	1.114
hPEO (40 kDa)	$39._2$	1.01	890	-	1.114
dPEO (20 kDa)	$22._3$	1.03	470	99.7	1.215
dPEO (40 kDa)	$39._3$	1.01	826	99.0	1.215

a) Determined *via* SEC with MALS
b) Degree of polymerization based on a reference volume of v_{EO}
c) Determined *via* ^{1}H NMR spectroscopy and SEC with MALS
d) From ref. 24 at 90 °C, and neglecting any molar volume change for deuterated polymer.

Sample Preparation. To prepare dPEO/hPEO/salt blends, stock solutions of polymer and salt were prepared separately in acetonitrile and combined in the desired volume ratios to obtain specific salt concentrations. A rotary evaporator removed most of the solvent, and the samples were dried in a vacuum oven at 40 °C for 72 h and 90 °C for 24 h. All the samples were kept in a glovebox before use.

Small-Angle Neutron Scattering (SANS). Samples were loaded into appropriate sample cells for SANS measurement on the GP-SANS CG-2 beamline at the High Flux Isotope Reactor (HFIR), Oak Ridge National Laboratory (ORNL) in Oak Ridge, Tennessee, or the NG-B and NG-7 30m beamlines at the National Institute of Standards and Technology (NIST) in Gaithersburg, Maryland.[28] Portions of the experiments were conducted on the USANS instrument at NIST.[29] At ORNL, samples were melted into 19 mm inner diameter, 0.81 mm thick stainless-steel spacers on top of 1-in diameter quartz plates (Esco Optics) at 70 °C. The spacers were clamped on the quartz plates to avoid polymer leakage. Samples were annealed at 70 °C in a vacuum oven for 12 h before being taken out and putting another quartz plate on top of the polymer quickly. Before SANS measurement, the sample cells were sealed with o-rings and loaded into copper sample holders and preheated at 90 °C for at least 12 h in a vacuum oven. At NIST, samples were slowly melted into quartz banjo cells (Hellma) with 1 mm path length and degassed under vacuum at 90 °C for at least 48 h. Before measurements, the sample cells were loaded into titanium holders and preheated at 90 °C for at least 12 h in a vacuum oven. At ORNL, the neutron wavelength was λ = 4.75 Å with spread $\Delta\lambda/\lambda$ = 0.13, and three configurations with sample-to-detector distances of 1.8, 8.8, and 19.2 m were used to cover the scattering wavevector q range 0.003 − 0.4 $Å^{-1}$. At NIST, λ = 6.0 Å with spread $\Delta\lambda/\lambda$ = 0.14, and three configurations with sample-to-detector distances of 1, 4, and 13 m were used to cover the same q range. All measurements were conducted at 90 °C in a N_2 atmosphere, and the total scattering cross sections were calibrated by either water (ORNL) or the attenuated incident beam (NIST), and corrected for empty cell scattering, sample transmission, thickness, and detector sensitivity. The azimuthally isotropic two-dimensional (2D) scattering

patterns were then reduced to one-dimensional (1D) intensity I as a function of q.[30] The incoherent background scattering from hPEO-salt and dPEO-salt blends was measured separately.

RESULTS

Measuring the single-chain conformation of a polymer melt by SANS is straightforward in principle, when a matched pair of "normal" (h) and perdeuterated (d) polymers are available. However, adding salt to h/d polymer blends can introduce complications that interfere with the analysis, mainly due to uncertainties introduced in both the low q and high q scattering intensities. There are three main ways to analyze the SANS data, which differ in the emphasized q range and the reliance on assumptions.[31]

(1) Guinier analysis: The initial slope of a plot of ln $I(q)$ *vs.* q^2 is $-R_g^2/3$. This has the distinct advantage that R_g can be determined in a model-independent way, but the desirable range of a typical Guinier plot is approximately $qR_g \leq 1$. This requires the low q scattering intensity to be accurate, and any extra coherent scattering, for example, a commonly observed low q upturn, can interfere with the analysis.

(2) Random Phase Approximation (RPA) analysis: This approach utilizes data over the entire q range, but can, therefore, be sensitive to problems at either high or low q. It also makes the assumption that the chains are Gaussian over the entire fitting range.

(3) Kratky analysis: This approach focuses on the intermediate q range, and in particular, the fractal regime. By plotting q^2I *vs.* q (Kratky plot), the conformation of polymer chains can be determined: Gaussian coils saturate to a plateau value, while rigid rods increase linearly. Note that for random coils, this analysis should focus on the range $ql \leq 1$, where l is the statistical segment length, as the derivation of the Debye function (i.e., scattering function for a Gaussian coil) invokes this constraint.[32,33] This approach reduces any potential problems in determining the scattering intensity at extremely low and high q regions.

In the remainder of the paper, we will derive conformational information using Kratky analysis, and then further examine problems with SANS measurements of both salt-free and salt-doped PEO blends.

SANS profiles of salt-free dPEO/hPEO blends. Three different dPEO/hPEO blends with volume ratios 25/75, 50/50, and 75/25 were prepared, and the measured absolute scattering profiles are shown in Figures 1a and 1c (blends with 20 kDa and 40 kDa PEO, respectively). The scattering profiles for the pure component polymers are also shown. All the blend scattering profiles have the expected Debye-type shape but flatten out at high q, mainly due to the incoherent contribution. The 20 kDa blends demonstrate a significant upturn in the range $q < 0.01$ Å^{-1}, while those for 40 kDa do not. The pure deuterated polymers show a strong coherent scattering at low q; the hPEO samples do as well but to a much smaller extent. This phenomenon remains unexplained but has been noted by several authors in several different systems.[23,34,35,36] It is also conceivable that it has been seen in many other systems, but not reported or noted in the associated publications. It is not due to isotope distribution along the chain,[37] as these polymers are fully deuterated, and it is not due to chemical contaminants (see subsequent discussion). Clearly, this contribution can interfere with reliable low q fitting of the blends. Note that absent a clear explanation, it is not justified to subtract this coherent contribution from the blend scattering, as the effect may well not be additive. In fact, Figures 1a and 1c suggest this; while the dPEO scattering at low q is actually stronger for 40 kDa than 20 kDa, the 40 kDa blends show no obvious upturn. Similarly, the magnitude of the upturn in the 20 kDa blends varies with composition, but not systematically with dPEO content.

Considering now the high q region of the scattering, the background (attributed mainly to the incoherent scattering of the hPEO) becomes substantial, exceeding the coherent scattering from the blends themselves around $q \approx 0.2 - 0.3$ Å^{-1}. Thus, uncertainty in the value of the incoherent contribution can play a significant role, as is well known. In this work, we will consider three different ways to estimate this contribution, especially in the presence of added salt. A standard approach is to subtract the composition-weighted measured high q plateau values obtained for the

pure components. These values are collected in Table 2, as I_b^{meas}. A second, empirical approach is to use a single Debye function (or other appropriate function, depending on the system) with addition of a constant baseline (eq 1) to fit the measured intensity. In eq 1, the first term is the coherent scattering of a Gaussian coil where $x = q^2R_g^2$. The baseline term B accounts for the background scattering of various origins; in neutron scattering, it is mainly due to the incoherent contribution from the polymers (both hPEO and dPEO), but also includes a diffuse coherent contribution.

$$I(q,r) = \frac{2}{x^2}(x - 1 + \exp(-x)) + B \tag{1}$$

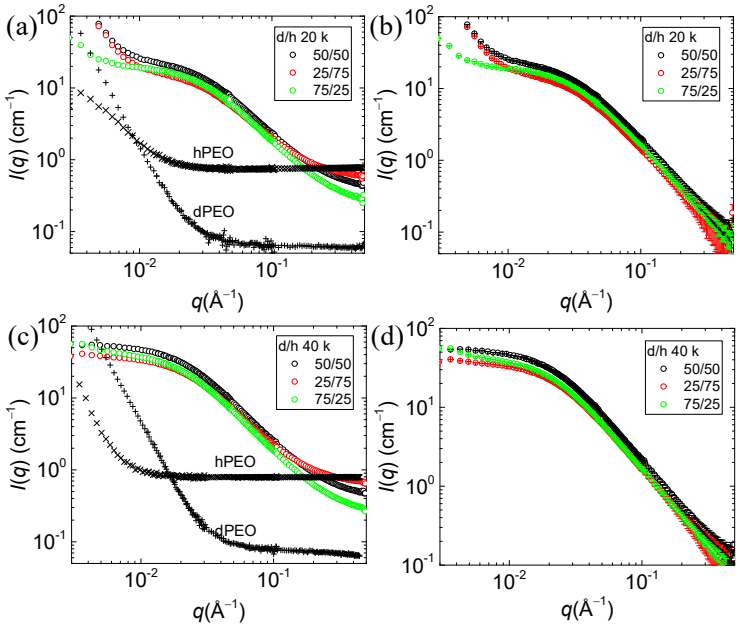

Figure 1: Absolute SANS profiles at 90 °C for salt-free dPEO/hPEO blends before (a, c) and after (b, d) incoherent background subtraction of 20 kDa and 40 kDa at varying volume ratios. The scattering profiles of pure hPEO and dPEO were demonstrated as × and +, respectively.

The values of B thus determined agree with I_b^{meas} for the salt-free blends to within about 10% (see Table 2), which is probably about the best that can be expected. Note that this agreement does not hold in the presence of salt, as will be discussed subsequently. After subtracting the B term from the measured intensity, the coherent scattering profiles are shown in Figures 1b and 1d. The

error bars are estimated from an assumed ±10% inaccuracy of B. We then analyze the coherent scattering from the blends.

From the RPA model, the structure factor of a binary blend with no interactions is given by

$$S(q) = \frac{I_{\mathrm{coh}}(q)}{\left(\frac{b_1}{v_1} - \frac{b_2}{v_2}\right)^2} = v_0 \left(\frac{1}{\phi_{\mathrm{D}} N_{\mathrm{D}} g\left(x_{\mathrm{D}}\right)} + \frac{1}{\left(1-\phi_{\mathrm{D}}\right) N_{\mathrm{H}} g\left(x_{\mathrm{H}}\right)} \right)^{-1} \tag{2}$$

where $\phi_{\mathrm{D}} = f\phi_{\mathrm{p}}$, $\phi_{\mathrm{H}} = (1-f)\phi_{\mathrm{p}}$, and f and ϕ_{p} are the volume fraction of dPEO in the polymer and the total volume fraction of polymer in the blends, respectively. Neutron scattering contrast is derived from the difference in the scattering length density b_i/v_i between the deuterated and protonated components. When analyzing blends with salt subsequently, the reference volume $v_0 = \bar{v}_{\mathrm{PEO}}$ represents the partial molar volume of PEO repeat units in the polymer/salt blends. In the case of LiTFSI-doped PEO, $\bar{v}_{\mathrm{PEO}}$ as a function of r was determined by Loo, et al.[24] accounting for non-ideal mixing, and in the case of $LiClO_4$-doped PEO, v_0 is taken to be v_{PEO}, assuming ideal mixing. N_i is the degree of polymerization of polymer, and $g(x_i)$ is the Debye function of the polymer chain. The R_g for protonated and deuterated PEO follows eq 3.

$$R_{\mathrm{g,D}} = \left(\frac{N_{\mathrm{D}}}{N_{\mathrm{H}}} \right)^{1/2} R_{\mathrm{g,H}} \tag{3}$$

Note that in eq 2, the contribution of salts can be neglected since salt ions are evenly distributed in hPEO and dPEO. The Flory-Huggins interaction parameter between PEO and salts is also neglected. At 90 °C, the isotopic interaction parameter between hPEO and dPEO is estimated to be 5×10^{-4} based on the monomer reference volume, with bond polarizabilities taken from the

literature.[34,38,39] Even for the 40 kDa blends, the isotropic interaction parameter can, therefore, be neglected. To simplify the calculation, we further assume $N_D = N_H = \left[M_n(\text{hPEO})M_n(\text{dPEO})\right / M_{hEO}M_{dEO}\right]^{1/2}$. Thus the structure factor can be determined as shown in eq 4, and in the limit of large q, while maintaining $ql < 1$, the product of $q^2S(q)$ (the Kratky form) can be calculated *via* eq 5, which is q-independent for random coils. This is reflected in the Kratky plots of $q^2S(q)$ *vs.* q, where high q plateaus are observed (Figures 2a and 2c). The Kratky intensity can be normalized accounting for the volume fractions of hPEO and dPEO, and then the plateau value is determined only by the statistical segment length (l) (eq 6).

$$\frac{S(q)}{v_0} = \phi_p f(1-f) N g(x) \tag{4}$$

$$\frac{q^2 S(q)}{v_0} = \phi_p f(1-f) N \frac{2}{R_g^{\,2}} = \frac{12\phi_p f(1-f)}{l^2} \tag{5}$$

$$\frac{q^2 S(q)}{v_0 \phi_p f(1-f)} = \frac{12}{l^2} \tag{6}$$

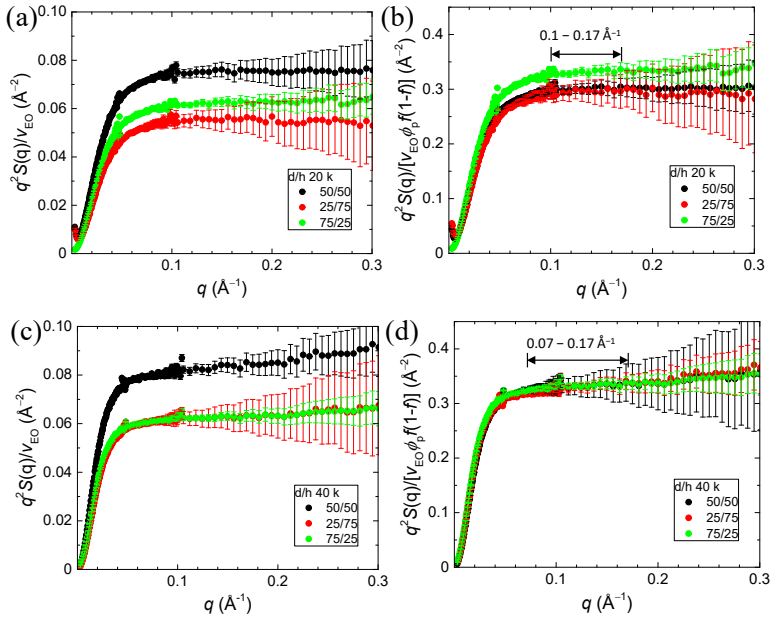

Figure 2: (a, c) Kratky plots and (b, d) normalized Kratky plots for salt-free dPEO/hPEO blends (kDa and 40 kDa at varying volume ratios. The arrows demonstrate the selected q ranges that used determine l. The error bars reflect an assumed 10% uncertainty in the background subtraction.

For the salt-free PEO blends, the normalized Kratky intensities are shown in Figures 2b and 2d. They reach a plateau with almost constant values, which were determined over the range of 0.10 Å^{-1} < q < 0.17 Å^{-1} (20 kDa) and 0.07 Å^{-1} < q < 0.17 Å^{-1} (40 kDa), respectively. The statistical segment lengths can be derived from the fits of the Kratky asymptotes as a function of dPEO fraction (f) (Figure S11).[40] The resulting statistical segment lengths are l = 6.25 ± 0.10 Å (20 kDa) and 6.07 ± 0.02 Å (40 kDa). These values agree well with recent literature,[22,24,41,42,43] as will be discussed subsequently. The increasing uncertainty in the background subtraction at higher q is also clearly evident in these plots, but it is important to reiterate that there is no *a priori* reason to expect the Kratky plateau to persist for ql > 1.

Table 2. Background Scattering of Polymer Blends With and Without Salt.

Salt		r	ϕ_{salt}	B (cm^{-1})[a]	I_b^{meas} (cm^{-1})[b]	I_{incoh}^{cal} (cm^{-1})[c]	I_{diff}^{cal} (cm^{-1})[d]
Neat	d/h 25/75	0	0	0.540	0.580	0.314	0.050
	d/h 50/50			0.358	0.407	0.213	0.066
	d/h 75/25			0.213	0.234	0.111	0.050
LiTFSI		1/64	0.0579	0.354	0.389	0.201	0.067
		1/32	0.104	0.349	0.373	0.191	0.068
		1/24	0.130	0.323	0.363	0.186	0.069
		1/15	0.182	0.265	0.345	0.175	0.072
		1/8	0.264	0.164	0.313	0.158	0.078
$LiClO_4$		1/64	0.0173	0.364	0.397	0.210	0.065
		1/15	0.0700	0.276	0.378	0.199	0.062
		1/8	0.124	0.255	0.359	0.189	0.058
LiI		1/15	0.0524	0.278	-	0.202	0.067

a) The term B in eq 1.
b) Determined from Figure S7 and eq 7.
c) Calculated using eq 8.
d) Calculated using eq 9.

SANS profiles of salt-doped hPEO/dPEO blends. Having established a reasonable and consistent analysis of the salt-free blends, we now turn to the influence of salt. LiTFSI-doped blends (r = 1/64, 1/32, 1/24, 1/15, 1/8) and $LiClO_4$-doped blends (r = 1/64, 1/15, 1/8) were prepared with a dPEO/hPEO ratio of 50/50, and the coherent scattering was determined by the same empirical method as above. The results are plotted in Figure 3. A low q upturn is apparent in many blends and is particularly severe in $LiClO_4$-doped blends with r = 1/64, for both molecular weights. One might even attribute this strange behavior to a problem with the sample, but as it holds for both molecular weights, this seems improbable. A candidate explanation could invoke inhomogeneity of the distribution of $LiClO_4$, but then it would be hard to explain why adding more salt makes the upturn much less pronounced. In any case, the low q upturn in salty blends makes it challenging to derive the chain conformation information by either Guinier analysis or by fitting to the RPA, both of which rely on the low q signal. In comparison, Kratky analysis, which only

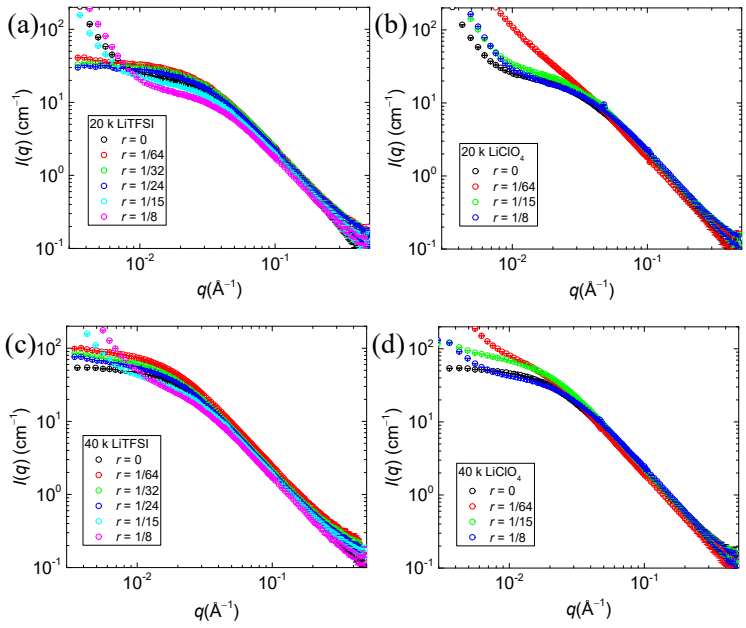

Figure 3: Coherent SANS intensity at 90 °C for dPEO/hPEO blends (50/50) doped with (a, c) LiTFSI and (b, d) $LiClO_4$ for (a, b) 20 kDa and (c, d) 40 kDa.

requires information at intermediate q, can still be applied to determine the statistical segment length (l).

When the blends are doped with salt, the normalized Kratky plateau intensity varies. For the LiTFSI-doped blends, the intensity increases even at the lowest salt doping (r = 1/64), while further increases in salt concentration do not result in an evident change in the intensity (Figures 4a and 4c). For the $LiClO_4$-doped blends, the plateau intensity decreases slightly at the lowest salt doping but increases at higher salt concentrations (Figures 4b and 4d). Since the plateau intensity is inversely proportional to l^2, the statistical segment length decreases and then stays almost constant with r when doped with LiTFSI but increases slightly and then decreases with r when doped with $LiClO_4$.

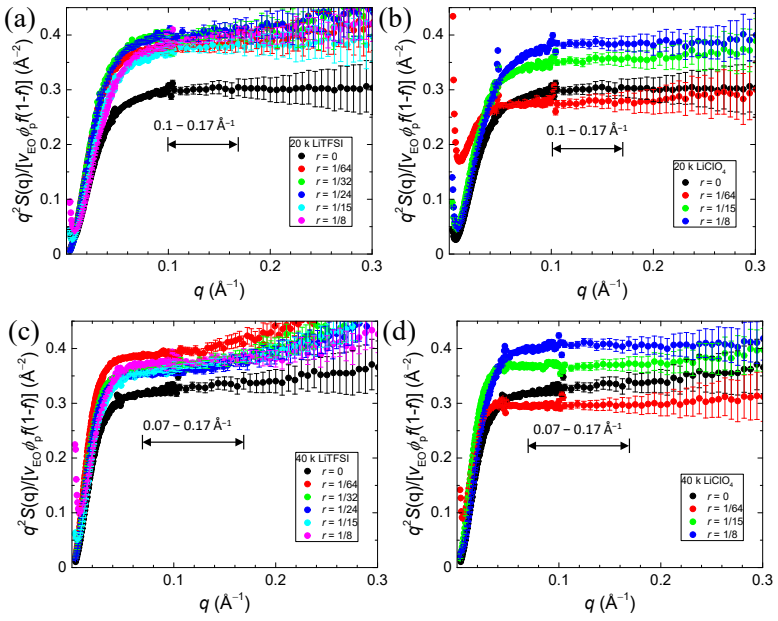

Figure 4: Normalized Kratky plots for dPEO/hPEO blends (50/50) doped with (a, c) LiTFSI and (b, d) $LiClO_4$ for (a, b) 20 kDa and (c, d) 40 kDa. The arrows indicate the q ranges used to determine l. The error bars reflect an assumed 10% uncertainty in the background subtraction.

DISCUSSION

Comparison with results from the literature. The calculated *l* values are plotted and compared with results from the literature in Figure 5a. Investigations of PEO chain conformations date back to the 1980s when Kugler et al. first studied dPEO/hPEO blends with different compositions by SANS, and *l* was determined to be 6.7 Å at 80 °C.[41] Subsequently, Smith et al. studied the same system, and found 5.9 Å,[42] while Fetters et al. report a value of 6.0 Å at 140 °C.[43] More recently, Annis et al. reported *l* to be 5.9 Å,[22] while Loo et al. reported 6.3 Å at 90 °C (data shown in Figure 5a).[24] Although PEO melts may exhibit a negative temperature coefficient of chain dimensions,[42] the differences in *l* are likely within the uncertainty of SANS experiments. By taking the average of all the data from literature and the current study, $l = 6.2 \pm 0.3$ Å (5% error in a SANS experiment), shown as the arrow in Figure 5a. In the current system, LiTFSI-doped blends demonstrate a *ca.* 9% decrease in *l* even at the lowest $r = 1/64$, and then *l* stays at an almost constant value of 5.6 Å up to $r = 1/8$, and the 40 kDa blends show a slightly larger *l* at higher *r*. In comparison, Loo et al. reported that in the range of $r < 0.1$, *l* decreases linearly with *r*, and *r* needs to exceed 0.03 to reach a 10% decrease, and a maximum reduction of *ca.* 19% in *l* occurs at $r = 0.125$ if the trend

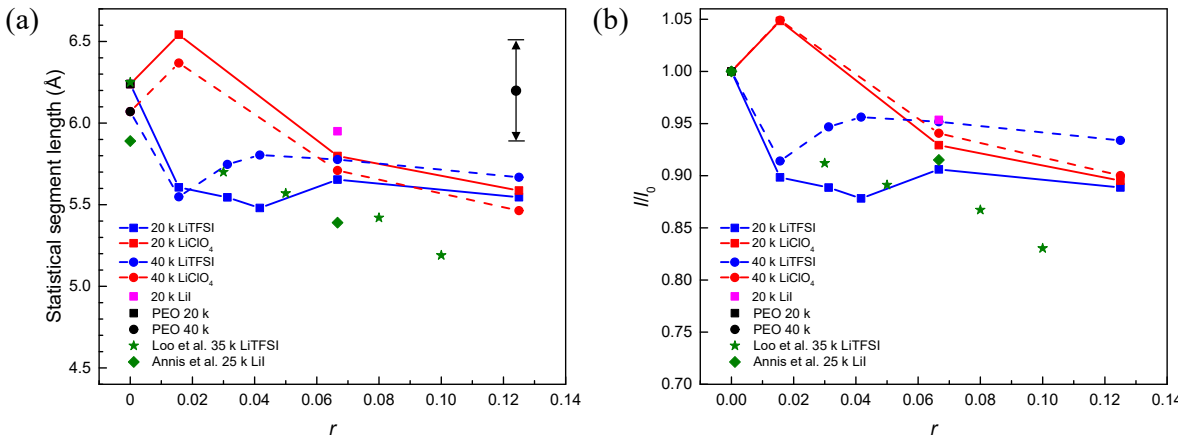

Figure 5: (a) Statistical segment length (*l*) of salt-doped dPEO/hPEO blends at 90 °C as a function of salt concentration. The black arrow illustrates the estimated uncertainty of *l* for salt-free PEO. (b) The ratio of *l* of salt-doped to the salt-free blends (l/l_0). *l* was calculated according to eq 6 from the normalized Kratky plateau values. The data reported by Annis et al. (Ref. 22) (green dimonds) and Loo et al. (Ref. 24) (green stars) are included for comparison.

continues.[24] All these results support the idea that the strong interaction between ether oxygens and lithium cations leads to a contraction in the PEO chain conformation, but the magnitude differs. Our system demonstrates a slightly weaker effect than Loo et al., except at the lowest concentration.

It is also worth noting that Annis et al. observed a decrease of *ca.* 9% in l for LiI-doped blends at r = 1/15, similar to the effect of LiTFSI at the same salt concentration. However, the absolute l values of the neat and salt-doped blends are lower than the current system. For comparison, we also studied a LiI-doped blend (20 kDa, r = 1/15), but l only decreases by 5% to 5.95 Å. We speculate that the weaker effect of LiI is related to the ion-pair formation mechanism. It is known that metal halides tend to bond strongly in a polymer matrix, and less than 1% of NaI is in the form of free ions in PEO at r = 1/250.**Error! Bookmark not defined.**

The trend of $LiClO_4$-doped blends in the current system is a little surprising. At r = 1/15 and 1/8, the decrease is somewhat similar to that of LiTFSI-doped blends, but at r = 1/64, a 5% increase is observed for both molecular weights. We are not aware of any mechanism that leads to an increase of l with the addition of salt. Note that at this salt concentration, the measured scattering profiles demonstrate the most substantial upturn at low q (Figures 2b and 2d), the origin of which is also uncertain. Further studies with low concentrations of $LiClO_4$ may be warranted.

Low q upturn in polymer blends. Since SANS became popular in polymer science in the 1980s, one persistent problem is unwanted coherent scattering at low q, which potentially causes inaccuracy in data analysis. For example, Bates et al. found that perdeuterated and protonated poly(vinylethylene) and poly(ethylethylene) have low q coherent scattering at $q < 0.015$ Å^{-1}, which was tentatively ascribed to the residual catalyst.[34] Similarly, Zeng, et al. observed an upturn in both deuterated and protonated saturated polybutadienes, where the deuterated polymer has a more substantial upturn.[36] Fullerton-Shirey and Maranas observed this phenomenon at $q < 0.02$ Å^{-1} in both salt-free and $LiClO_4$-doped hPEO,[35] and Triolo, et al. reported similar effects at $q < 0.06$ Å^{-1} in salt-free and LiI-doped dPEO, where the absolute intensity is higher for dPEO than hPEO.[23] As we speculated before, it is quite conceivable that many other observations of this effect have gone

unreported. To date, multiple hypotheses have been considered to explain the low q upturn feature; it is possible that the main factor might differ from case to case. The most common conjecture is an impurity introduced in the synthesis and purification steps (catalysts, salts, and dust), which results in extra particle scattering. Given the occurrence and the magnitude of the effect in completely different chemical systems, this seems unlikely. Similarly, imperfections in sample windows seem unlikely. Another possibility is tiny voids due to inefficient degassing, which might be more pronounced in high-T_g polymers. Allen and Tanaka drew this conclusion as far back as 1978 for the particular case of dPEO.[44] Moreover, in the case of a hygroscopic polymer such as PEO, water clusters might form to different degrees.[35] Also, Hammouda, Ho, and Kline found a significant amount of PEO clusters in deuterated benzene and deuterated water, attributable to hydrogen bonding and hydrophobic interactions.[45,46,47] A further possibility is chain aggregation driven by end groups, although this seems improbable given the high molecular weight of the polymer and the small size of the *tert*-butoxy and hydroxyl end groups; such end group effects have been observed in PEO solutions.[46] Given the fact that the amount and size of clusters increase as the concentration of PEO increases,[48] it is conceivable that trace amounts of water in the PEO melt act as a crosslinker to form clusters. However, there is no evidence of a peak in the Kratky plots in Figure 2, which would be suggestive of a star-like form factor. Finally, instrumental artifacts have not been ruled out.

To explore this problem further, we measured the SANS profiles of hPEO and dPEO (20 kDa) at both ORNL and NIST (Figure S4). At both facilities, the high q incoherent scattering intensities are essentially the same for both hPEO and dPEO, while the low q upturn intensities are different. At ORNL, the intensity decays as $q^{-1.1}$ and $q^{-2.4}$ for hPEO and dPEO, respectively, while at NIST, the decays follow $q^{-3.6}$ and $q^{-3.4}$, respectively. Note that the polymers are synthesized and purified by the same method, and the only difference is the sample cell used on the SANS instrument. The modest discrepancy might result from inadequate degassing. At ORNL where samples were degassed on quartz plates in spacers, any moisture and trapped air bubbles can be removed more

efficiently, while at NIST where samples were degassed in banjo cells with a tiny opening, this process is less efficient. Moreover, we heated the hPEO and dPEO samples at elevated temperatures up to 170 °C on the beamline at NIST, trying to decrease the number of voids, but the low q SANS data remained identical (Figure S5). We also studied the coherent scattering of LiTFSI-doped dPEO over an extended q range by a combination of SANS and USANS at NIST (Figure 6), and the upturn is confirmed down to at least $q \approx 3 \times 10^{-5}$ Å^{-1}. This agreement among different instrumental configurations argues strongly against an instrumental artifact. We, therefore, take inadequate degassing ("voids") as the most likely explanation. Micro voids can produce strong scattering at low q, due to the strong scattering length density (SLD) difference between polymer matrix and voids, as has also been observed in small-angle X-ray scattering (SAXS). The sizes of the micro voids exceed the detection range of small-angle scattering techniques. Thus, the low q upturn in SANS or SAXS could be attributed to the scattering from the surfaces. For objects with sharp interfaces, this would produce a q^{-4} asymptote, i.e., Porod's law. In practice, deviations from the Porod's law are often observed due to the fuzzy interface (or transition layer) or density fluctuations.[49] This picture is consistent with the low q asymptotes observed in the NIST data, as discussed above. We estimated the volume fraction of voids by a polydisperse sphere model,[50] assuming that the voids have a mean radius of 1 μm and a dispersity of 0.5, and fixing the contrast between void and dPEO-LiTFSI with $r = 1/64$. It was found that the calculated scattering pattern with a volume fraction ≈ 0.005 agreed with the experimental data in the range of $q > 0.002$ Å^{-1}, while overestimating the scattering intensity in the ultra-low q range (Figure S12). The prefactor in the Porod's law is associated with the specific surface area. Therefore, as the micro voids shrink, the strength of the low q upturn decreases, and the asymptote becomes less pronounced. This could explain why better degassing can mitigate the problem. However, one should bear in mind that complete removal of air trapped in viscous polymers is challenging. The low q upturn can make it difficult to obtain R_g using the Guinier method, but its influence on the Kratky analysis should be negligible, as the scattering from a Gaussian coil scales

with q^{-2}, while the low q upturn decays much more rapidly. In Kratky analysis, the correct subtraction of high q background becomes essential, as will be discussed later.

The neutron SLD of dPEO and hPEO are 7.08×10^{-6} and 6.40×10^{-7} Å^{-2}, respectively, and if we assume the voids are vacuum (SLD = 0), dPEO has a higher contrast with voids, resulting in a higher low q coherent scattering intensity. The fact that deuterated polymers (including dPEO) usually have a stronger low q coherent scattering than the hydrogenous polymers makes it possible to alleviate the effect by reducing the deuterated polymer composition in the blends; this strategy was adopted by Loo, et al.[24]

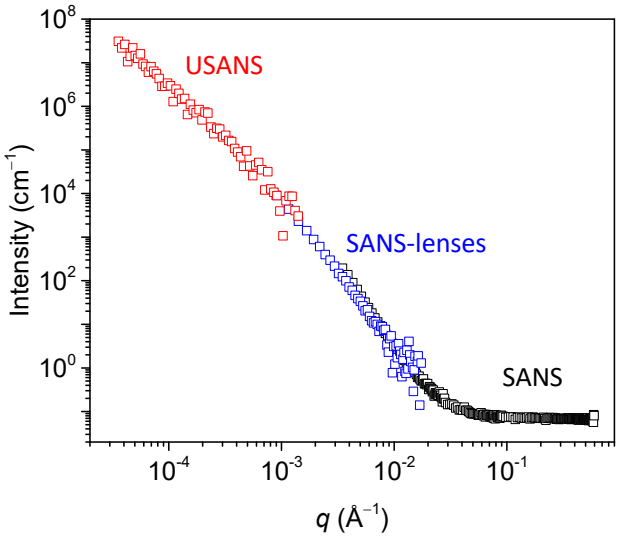

Figure 6: SANS from dPEO (40 kDa) with added LiTFSI (r = 1/64) with three different instruments at NIST, showing the persistence of the effect across configurations. Data in black were collected using the three configurations described in the experimental section, while data in blue were collected at a sample-to-detector distance of 15.3 m with λ = 8 Å and with lenses inserted. Data in red were collected on the USANS instrument.

Background subtraction in SANS. To obtain accurate coherent scattering from polymer blends, any unwanted scattering (scattering at high q and extra coherent scattering at low q) from hPEO and dPEO and the salts need to be addressed appropriately. Since ions can be well solvated in PEO, to investigate the influence of salt on hPEO and dPEO, the SANS profiles of salt-doped pure

polymers as a function of *r* were obtained (Figure S6). Note that the incoherent background for polymer blends varies with temperature (as shown in Figure S5), not only due to changes in density but also thermal motion, so all the measurements were conducted at 90 °C. Interestingly, the low *q* coherent scattering slope remains almost constant for both salt-doped hPEO and dPEO, which indicates that the salt itself does not make a significant contribution to the upturn in the blends. Since we rely on Kratky analysis to determine *l*, the impact of the unwanted scattering in the low *q* range is diminished, so here we focus on the high *q* scattering. For salt-doped dPEO, the experimental high *q* intensity remains constant with increasing *r*, which is due to the similarity of the total scattering intensity of dPEO and salt (Figure S6). In the case of salt-doped hPEO, the intensity first increases then decreases for both LiTFSI and $LiClO_4$ (Figure S7). The incoherent scattering intensity of these salts is lower than hPEO, thus increasing the amount of salt should reduce the background. We have no explanation of the abnormal increase at the lowest salt concentration, but we can use the data to estimate the background scattering in the salt-doped hPEO/dPEO blends at each salt concentration using eq 7.

$$I_{\mathrm{b}}^{\mathrm{meas}}(r) = fI_{\mathrm{b}}^{\mathrm{meas}}(\mathrm{dPEO-salt}, r) + (1-f)I_{\mathrm{b}}^{\mathrm{meas}}(\mathrm{hPEO-salt}, r) \tag{7}$$

Note that the scattering is the total scattering from the polymer and the salt, which contains both coherent and incoherent contributions. The incoherent scattering $I_{\mathrm{incoh}}^{\mathrm{cal}}$, can be calculated by the SLD calculator available from NIST using eq 8,[51]

$$I_{\mathrm{incoh}}^{\mathrm{cal}}(r) = \phi_{\mathrm{p}}(r)\left(fI_{\mathrm{incoh}}^{\mathrm{cal}}(\mathrm{dPEO}) + (1-f)I_{\mathrm{incoh}}^{\mathrm{cal}}(\mathrm{hPEO})\right) + (1-\phi_{\mathrm{p}}(r))I_{\mathrm{incoh}}^{\mathrm{cal}}(\mathrm{salt}) \tag{8}$$

while the coherent part, which is referred to as diffuse coherent scattering (DCS) $I_{\mathrm{diff}}^{\mathrm{cal}}$,[52,53] comes from the disordered scatterers in the system and is often ignored in the literature. Note that DCS

is associated with fluctuations, but it is coherent since it provides information about the disordered structure of the system, and diffuse because of the lack of q dependence. In SANS, by assuming a globally disordered system, i.e., no spatial correlationa among the scattering units, DCS can be calculated by eq 9

$$I_{\mathrm{diff}}^{\mathrm{cal}} = \frac{1}{2}\frac{V}{N}\sum_{\substack{\mathrm{i,j}\\ \mathrm{i}\neq\mathrm{j}}}^{m}\frac{\phi_{\mathrm{i}}\phi_{\mathrm{j}}}{v_{\mathrm{i}}v_{\mathrm{j}}}\left(\langle b_{\mathrm{i}}\rangle - \langle b_{\mathrm{j}}\rangle\right)^2 \tag{9}$$

where N scatterers are in a volume V, m is the number of types of scatterers, and ϕ_{i}, v_{i}, and $\langle b_{\mathrm{i}}\rangle$ are the volume fraction, volume, and scattering length of type i scatterer, respectively. The hEO, dEO monomers and the salt molecule can be regarded as the three types of scatterers involved in the system, and the values of $I_{\mathrm{diff}}^{\mathrm{cal}}$ for polymer blends with salt, and pure hPEO or dPEO with salt are summarized in Table 2 and Table S1. In heavily salt-loaded dPEO/hPEO blends, DCS makes up to 33% of the total background scattering ($I_{\mathrm{incoh}}^{\mathrm{cal}} + I_{\mathrm{diff}}^{\mathrm{cal}}$), and thus cannot be neglected in calculations.

As shown in Table 2, $I_{\mathrm{b}}^{\mathrm{meas}}(r)$ is larger than the value of the term B used in eq 1, especially for the heavily salt-loaded samples. On the other hand, the calculated background scattering intensity ($I_{\mathrm{incoh}}^{\mathrm{cal}} + I_{\mathrm{diff}}^{\mathrm{cal}}$) is lower than the term B used in eq 1. Note that the calculated scattering intensity is just an estimate, and thus we consistently adopted the value of term B in eq 1 as the background term for all the analysis throughout the paper. In particular the DCS calculated via eq 9 assumes completely random mixing, and is therefore a lower bound for this contribution. The discrepancy between $I_{\mathrm{b}}^{\mathrm{meas}}$ and B is more significant as r increases, possibly due to the excess DCS, but the absolute value of the difference ΔI is less than 0.15 cm^{-1}. In a typical normalized Kratky plot, this difference results in a deviation of less than 0.06 $\mathrm{Å}^2$, even at the high q limit (≈0.17 $\mathrm{Å}^{-1}$), which will lead to less than 10% error in the l determination. Since l is determined over a range of q, the high q deviation effect is weaker, and the estimated error is less than 5%.

Comparison with the RPA model. Using the l values obtained from the Kratky analysis, the theoretical scattering profiles of polymer blends can be predicted by the RPA (eq 2). The predicted and measured scattering profiles are plotted in Figures S8 and S9. Overall, the RPA predictions agree well with the measured data for $q > 0.03$ Å^{-1}.

CONCLUSIONS

The chain conformations in salt-free and salt-doped PEO melts have been studied by SANS at 90 °C, using two different molecular weights and two different salts. Due to the low q coherent scattering from pure hPEO and dPEO, and the inevitable uncertainty in the high q incoherent scattering, the statistical segment length is determined primarily by Kratky analysis using the intermediate q range. In general, the chain dimensions decrease with the addition of salt, and a roughly 10% decrease was observed at $r = 0.125$, for both molecular weights and for both salts. The effect of salt on the statistical segment length is compared with data from the literature, and where the systems overlap, the data agree reasonably well with prior results of Loo, et al. and Annis, et al. Furthermore, the scattering profiles were then calculated by the RPA and compared with the measured values, with satisfactory agreement found in all cases. Significant difficulties in data analysis, including an unexplained low q contribution for the pure polymers and the background scattering at high q, have also been discussed. The former is apparently ubiquitous in perdeuterated polymers, and remains unexplained. The data presented here argue against instrumental artifacts or impurities, thereby implicating "voids" as the most likely culprit. The high q scattering includes not only the incoherent contribution but also diffuse coherent scattering, which becomes more significant as the salt concentration increases.

DISCLAIMER

Certain commercial products or equipment are described in this paper to specify the experimental procedure adequately. In no case does such identification imply recommendation or

endorsement by the National Institute of Standards and Technology, nor does it imply that it is necessarily the best available for the purpose.

ACKNOWLEDGMENTS

This work was supported by the Office of Basic Energy Sciences (BES) of the U.S. Department of Energy (DoE), under Contract No. DE-FOA-0001664. Protonated and deuterated PEO were synthesized at the CNMS, which is a DOE Office of Science User Facility. This research used resources at the High Flux Isotope Reactor, a DOE Office of Science User Facility operated by the Oak Ridge National Laboratory. We acknowledge the support of the National Institute of Standards and Technology, U.S. Department of Commerce, in providing the neutron research facilities used in this work. Access to the USANS instrument was provided by the Center for High Resolution Neutron Scattering, a partnership between the National Institute of Standards and Technology and the National Science Foundation under Agreement No. DMR-1508249. S.X thanks Aaron Lindsay for proposing this study and acknowledges partial funding from a Doctoral Dissertation Fellowship at the University of Minnesota.

ASSOCIATED CONTENT

Supporting Information

The Supporting Information is available free of charge on the ACS Publications website at DOI: XXX.

SEC data of the polymers, additional SANS profiles of salt-doped pure hPEO, dPEO, and dPEO/hPEO blends, comparison of the result to RPA prediction, calculated scattering intensities of polymers and salts, background scattering intensities from Porod plots, Kratky asymptotes of salt-free blends, and estimated scattering from micro voids. (PDF)

REFERENCES

(1) Hickner, M. A. Ion-containing polymers: new energy & clean water. *Mater. Today* **2010,** *13*, 34-41.

(2) Fenton, D. E.; Parker, J. M.; Wright, P. V. Complexes of alkali metal ions with poly(ethylene oxide). *Polymer* **1973,** *14*, 589.

(3) Lascaud, S.; Perrier, M.; Vallee, A.; Besner, S.; Prud'homme, J.; Armand, M. Phase Diagrams and Conductivity Behavior of Poly(ethylene oxide)-Molten Salt Rubbery Electrolytes. *Macromolecules* **1994,** *27*, 7469-7477.

(4) Lassegues, J. C.; Grondin, J.; Talaga, D. Lithium solvation in bis(trifluoromethanesulfonyl)imide-based ionic liquids. *Phys. Chem. Chem. Phys.* **2006,** *8*, 5629-5632.

(5) Dou, S.; Zhang, S.; Klein, R. J.; Runt, J.; Colby, R. H. Synthesis and Characterization of Poly(Ethylene Glycol)-Based Single-Ion Conductors. *Chem. Mater.* **2006,** *18*, 4288-4295.

(6) Xue, Z.; He, D.; Xie, X. Poly(ethylene oxide)-based electrolytes for lithium-ion batteries. *J. Mater. Chem. A* **2015,** *3*, 19218-19253.

(7) Virgili, J. M.; Hexemer, A.; Pople, J. A.; Balsara, N. P.; Segalman, R. A. Phase Behavior of Polystyrene-block-poly(2-vinylpyridine) Copolymers in a Selective Ionic Liquid Solvent. *Macromolecules* **2009,** *42*, 4604-4613.

(8) Park, M. J.; Balsara, N. P. Phase Behavior of Symmetric Sulfonated Block Copolymers. *Macromolecules* **2008,** *41*, 3678-3687.

(9) Wanakule, N. S.; Virgili, J. M.; Teran, A. A.; Wang, Z.-G.; Balsara, N. P. Thermodynamic properties of block copolymer electrolytes containing imidazolium and lithium salts. *Macromolecules* **2010,** *43*, 8282-8289.

(10) Teran, A. A.; Balsara, N. P. Thermodynamics of block copolymers with and without salt. *J. Phys. Chem. B* **2014,** *118*, 4-17.

(12) Sing, C. E.; Zwanikken, J. W.; Olvera de la Cruz, M. Electrostatic control of block copolymer morphology. *Nat. Mater.* **2014,** *13*, 694-698.
(13) Lee, H.-N.; Lodge, T. P. Lower critical solution temperature (LCST) phase behavior of poly(ethylene oxide) in ionic liquids. *J. Phys. Chem. Lett.* **2010,** *1*, 1962-1966.
(14) Lee, H.-N.; Newell, N.; Bai, Z.; Lodge, T. P. Unusual lower critical solution temperature phase behavior of poly(ethylene oxide) in ionic liquids. *Macromolecules* **2012,** *45*, 3627-3633.
(15) Kharel, A.; Lodge, T. P. Coil Dimensions of Poly(ethylene oxide) in an Ionic Liquid by Small-Angle Neutron Scattering. *Macromolecules* **2017,** *50*, 8739-8744.
(16) Kharel, A.; Lodge, T. P. Effect of Ionic Liquid Components on the Coil Dimensions of PEO. *Macromolecules* **2019,** *52*, 3123-3130.
(17) Chen, Z.; FitzGerald, P. A.; Warr, G. G.; Atkin, R. Conformation of poly(ethylene oxide) dissolved in the solvate ionic liquid [Li(G4)]TFSI. *Phys. Chem. Chem. Phys.* **2015,** *17*, 14872-14878.
(18) Chen, Z.; McDonald, S.; Fitzgerald, P. A.; Warr, G. G.; Atkin, R. Structural effect of glyme-Li(+) salt solvate ionic liquids on the conformation of poly(ethylene oxide). *Phys. Chem. Chem. Phys.* **2016,** *18*, 14894-14903.
(19) Müller-Plathe, F.; van Gunsteren, W. F. Computer simulation of a polymer electrolyte: Lithium iodide in amorphous poly(ethylene oxide). *J. Chem. Phys.* **1995,** *103*, 4745-4756.
(20) Rey, I.; Lassègues, J. C.; Grondin, J.; Servant, L. Infrared and Raman study of the PEO-LiTFSI polymer electrolyte. *Electrochim. Acta* **1998,** *43*, 1505-1510.
(21) Borodin, O.; Smith, G. D. Molecular Dynamics Simulations of Poly(ethylene oxide)/LiI Melts. 1. Structural and Conformational Properties. *Macromolecules* **1998,** *31*, 8396-8406.
(11) Sing, C. E.; Zwanikken, J. W.; Olvera de la Cruz, M. Ion Correlation-Induced Phase Separation in Polyelectrolyte Blends. *ACS Macro Lett.* **2013,** *2*, 1042-1046.

(22) Annis, B. K.; Kim, M. H.; Wignall, G. D.; Borodin, O.; Smith, G. D. A study of the influence of LiI on the chain conformations of poly(ethylene oxide) in the melt by small-angle neutron scattering and molecular dynamics simulations. *Macromolecules* **2000,** *33*, 7544-7548.

(23) Triolo, A.; Lo Celso, F.; Arrighi, V.; Strunz, P.; Lechner, R. E.; Mastragostino, M.; Passerini, S.; Annis, B. K.; Triolo, R. Structural and dynamical characterization of melt PEO–salt mixtures. *Physica A: Statistical Mechanics and its Applications* **2002,** *304*, 308-313.

(24) Loo, W. S.; Mongcopa, K. I.; Gribble, D. A.; Faraone, A. A.; Balsara, N. P. Investigating the Effect of Added Salt on the Chain Dimensions of Poly(ethylene oxide) through Small-Angle Neutron Scattering. *Macromolecules* **2019,** *52*, 8724-8732.

(25) Kamiyama, Y.; Shibata, M.; Kanzaki, R.; Fujii, K. Lithium-ion coordination-induced conformational change of PEG chains in ionic-liquid-based electrolytes. *Phys. Chem. Chem. Phys.* **2020,** *22*, 5561-5567.

(26) Ndoni, S.; Papadakis, C. M.; Bates, F. S.; Almdal, K. Laboratory-scale setup for anionic polymerization under inert atmosphere. *Rev. Sci. Instrum.* **1995,** *66*, 1090-1095.

(27) Brandrup, J.; Immergut, E. H.; Grulke, E. A.; Abe, A.; Bloch, D. R., *Polymer handbook*. Wiley New York etc: 1989; Vol. 7.

(28) Glinka, C. J.; Barker, J. G.; Hammouda, B.; Krueger, S.; Moyer, J. J.; Orts, W. J. The 30 m Small-Angle Neutron Scattering Instruments at the National Institute of Standards and Technology. *J. Appl. Crystallogr.* **1998,** *31*, 430-445

(29) Barker, J. G.; Glinka, C. J.; Moyer, J. J.; Kim, M. H.; Drews, A. R.; Agamalian, M. Design and performance of a thermal-neutron double-crystal diffractometer for USANS at NIST. *J. Appl. Crystallogr.* **2005,** *38*, 1004-1011

(30) Kline, S. R. Reduction and analysis of SANS and USANS data using IGOR Pro. *J. Appl. Crystallogr.* **2006,** *39*, 895-900.

(31) Hammouda, B. The SANS toolbox. *NIST Center for Neutron Research, Gaithersburg, MD, USA.* [Online] **2008**. https://www.ncnr.nist.gov/staff/hammouda/the_SANS_toolbox.pdf (accessed March 24, 2020)

(32) Altenberger, A. R.; Rosa, E.; Dahler, J. S. The static scattering function and optical birefringence of a deformed, ideal polymer chain. *J. Chem. Phys.* **1991,** *95*, 9248-9257.

(33) Debye, P. Molecular-weight determination by light scattering. *J Phys Colloid Chem* **1947,** *51*, 18-32.

(34) Bates, F. S.; Fetters, L. J.; Wignall, G. D. Thermodynamics of isotopic polymer mixtures: poly(vinylethylene) and poly(ethylethylene). *Macromolecules* **1988,** *21*, 1086-1094.

(35) Fullerton-Shirey, S. K.; Maranas, J. K. Effect of $LiClO_4$ on the Structure and Mobility of PEO-Based Solid Polymer Electrolytes. *Macromolecules* **2009,** *42*, 2142-2156.

(36) Zeng, Y.; López-Barrón, C. R.; Kang, S.; Eberle, A. P. R.; Lodge, T. P.; Bates, F. S. Effect of Branching and Molecular Weight on Heterogeneous Catalytic Deuterium Exchange in Polyolefins. *Macromolecules* **2017,** *50*, 6849-6860.

(37) Balsara, N. P.; Lohse, D. J.; Graessley, W. W.; Krishnamoorti, R. Small-angle neutron scattering by partially deuterated polymers and their blends. *J. Chem. Phys.* **1994,** *100*, 3905-3910.

(38) Bell, R. P. Polarisibility and internuclear distance. *Trans. Faraday Society* **1942,** *38*, 0422-0429.

(39) Bates, F. S.; Wignall, G. D. Isotope-induced quantum-phase transitions in the liquid state. *Phys. Rev. Lett.* **1986,** *57*, 1429-1432.

(40) Cabral, J. o. T.; Higgins, J. S. Small Angle Neutron Scattering from the Highly Interacting Polymer Mixture TMPC/PSd: No Evidence of Spatially Dependent χ Parameter. *Macromolecules* **2009,** *42*, 9528-9536.

(41) Kugler, J.; Fischer, E. W.; Peuscher, M.; Eisenbach, C. D. Small angle neutron scattering studies of poly (ethylene oxide) in the melt. *Die Makromolekulare Chemie: Macromolecular Chemistry and Physics* **1983,** *184*, 2325-2334.

(42) Smith, G. D.; Yoon, D. Y.; Jaffe, R. L.; Colby, R. H.; Krishnamoorti, R.; Fetters, L. J. Conformations and Structures of Poly(oxyethylene) Melts from Molecular Dynamics Simulations and Small-Angle Neutron Scattering Experiments. *Macromolecules* **1996,** *29*, 3462-3469.

(43) Fetters, L.; Lohse, D.; Richter, D.; Witten, T.; Zirkel, A. Connection between polymer molecular weight, density, chain dimensions, and melt viscoelastic properties. *Macromolecules* **1994,** *27*, 4639-4647.

(44) Allen, G.; Tanaka, T. A small-angle neutron scattering study on poly(ethylene oxide) crystals. *Polymer* **1978,** *19*, 271-276.

(45) Hammouda, B.; Ho, D.; Kline, S. SANS from Poly(ethylene oxide)/Water Systems. *Macromolecules* **2002,** *35*, 8578-8585.

(46) Hammouda, B.; Ho, D. L.; Kline, S. Insight into Clustering in Poly(ethylene oxide) Solutions. *Macromolecules* **2004,** *37*, 6932-6937.

(47) Ho, D. L.; Hammouda, B.; Kline, S. R. Clustering of poly(ethylene oxide) in water revisited. *J. Polym. Sci., Part B: Polym. Phys.* **2003,** *41*, 135-138.

(48) Polverari, M.; van de Ven, T. G. M. Dilute Aqueous Poly(ethylene oxide) Solutions: Clusters and Single Molecules in Thermodynamic Equilibrium. *J. Phys. Chem.* **1996,** *100*, 13687-13695.

(49) Ruland, W. Small-angle scattering of two-phase systems: determination and significance of systematic deviations from Porod's law. *J. Appl. Crystallogr.* **1971,** *4*, 70-73.

(50) Griffith, W. L.; Triolo, R.; Compere, A. L. Analytical scattering function of a polydisperse Percus-Yevick fluid with Schulz- (Gamma -) distributed diameters. *Phys Rev A Gen Phys* **1987,** *35*, 2200-2206.

(51) Kienzle P. Scattering Length Density Calculator [Online] https://www.ncnr.nist.gov/resources/sldcalc.html (accessed March 24, 2020)

(52) Glinka, C. J. Incoherent neutron scattering from multi-element materials. *J. Appl. Crystallogr.* **2011,** *44*, 618-624.

(53) Rathje, J.; Ruland, W. Density fluctuations in amorphous and semicrystalline polymers. *Colloid. Polym. Sci.* **1976,** *254*, 358-370.